Supplementary Materials

Simulation of Femtosecond Transient Absorption Spectra of a Perylene-Based Light Harvesting Antenna

Royle Perez-Castillo[a], Victor M. Freixas[b], Aliezer Martinez-Mesa[c], Llinersy Uranga-Piña[c,f], Maxim F. Gelin[d], Sergei Tretiak[e], Sebastian Fernandez-Alberti[a*]

[a]Departamento de Ciencia y Tecnologia, Universidad Nacional de Quilmes/CONICET, B1876BXD Bernal, Argentina
[b]Department of Chemistry and Physics and Astronomy, University of California, Irvine, California 92697-2025, United States.
[c]DynAMoS (Dynamical processes in Atomic and Molecular Systems), Facultad de Física, Universidad de La Habana, San Lázaro y L, La Habana 10400, Cuba.
[d]School of Sciences, Hangzhou Dianzi University, Hangzhou 310018, China.
[e]Theoretical Division, Center for Nonlinear Studies (CNLS), and Center for Integrated Nanotechnologies (CINT), Los Alamos National Laboratory, Los Alamos, NM 87545, USA
[f]Laboratoire Collisions Agrégats Réactivité (FeRMI), UMR 5589, Université de Toulouse, F-31062 Toulouse Cedex 09, France

*corresponding author: sfalberti@gmail.com

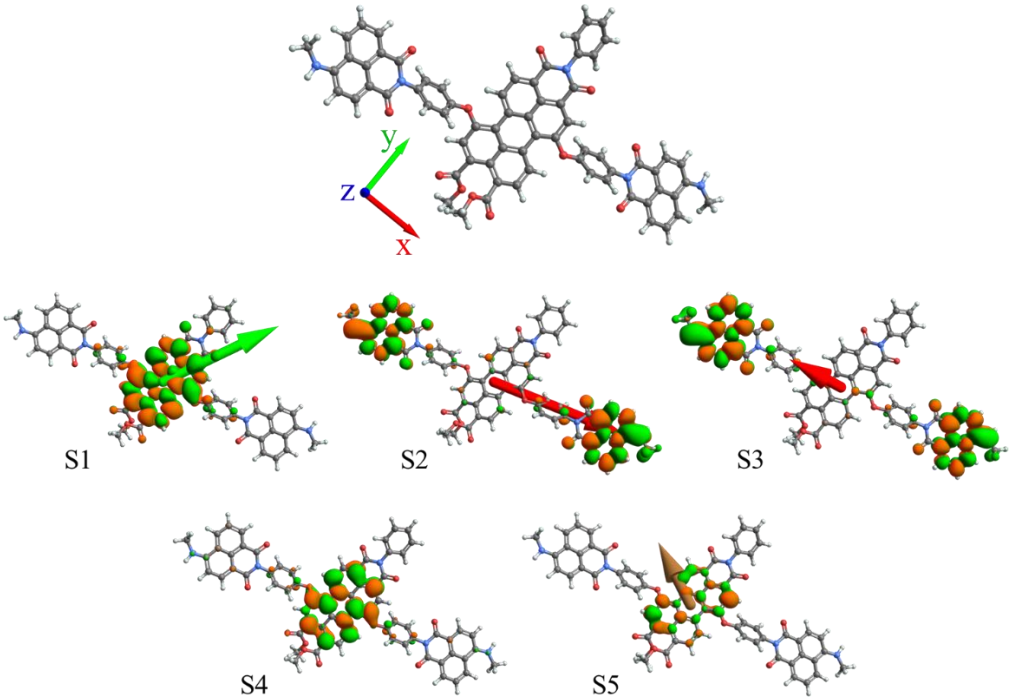

Figure S1. Chemical structure of the dendrimer T1 indicating the x, y, and z directions of the body-fixed reference frame. Spatial distributions of electronic transition densities indicating the orientation of their corresponding transition dipole moments (μ) for the five lowest energy electronic states.

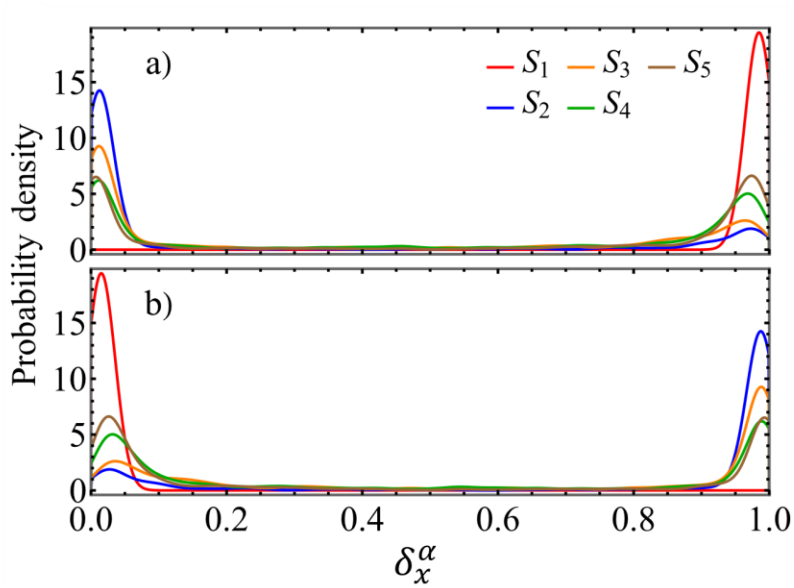

Figure S2. Distribution of the average fraction of the transition density matrix ($\delta_X^\alpha(t)$) localized on the (a) donors, and (b) acceptor chromophores evaluated from snapshots collected during a long-equilibrated ground state molecular dynamics simulation.

S_1

Hole Weight = 0.894923 Particle

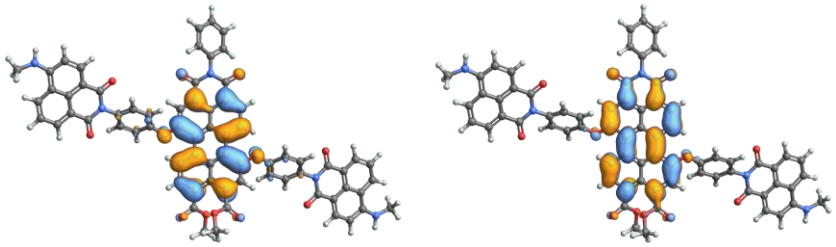

S_2

Hole Weight = 0.718553 Particle

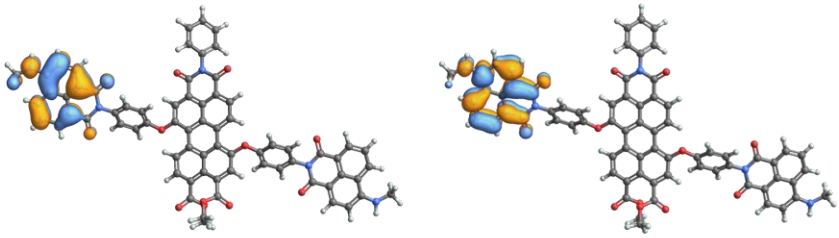

S_3

Hole Weight = 0.707879 Particle

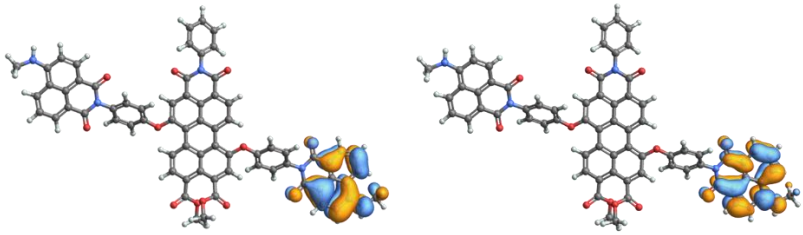

S_4

Hole Weight = 0.671476 Particle

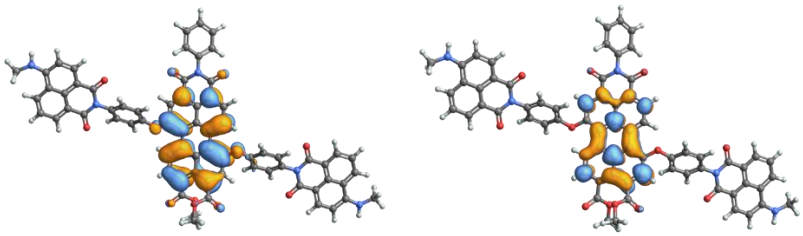

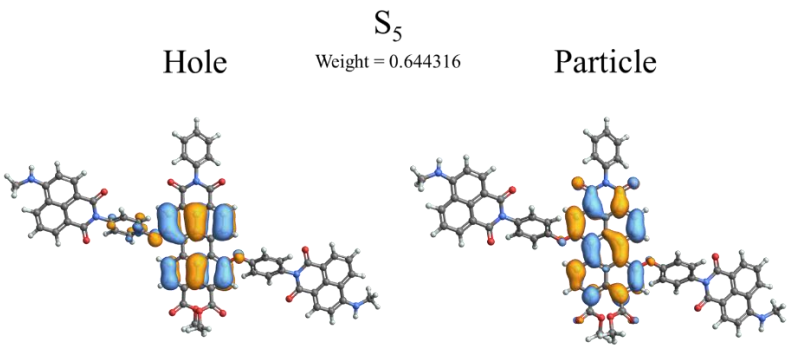

Figure S3. Hole-electron pairs calculated for the first 5 excited states.

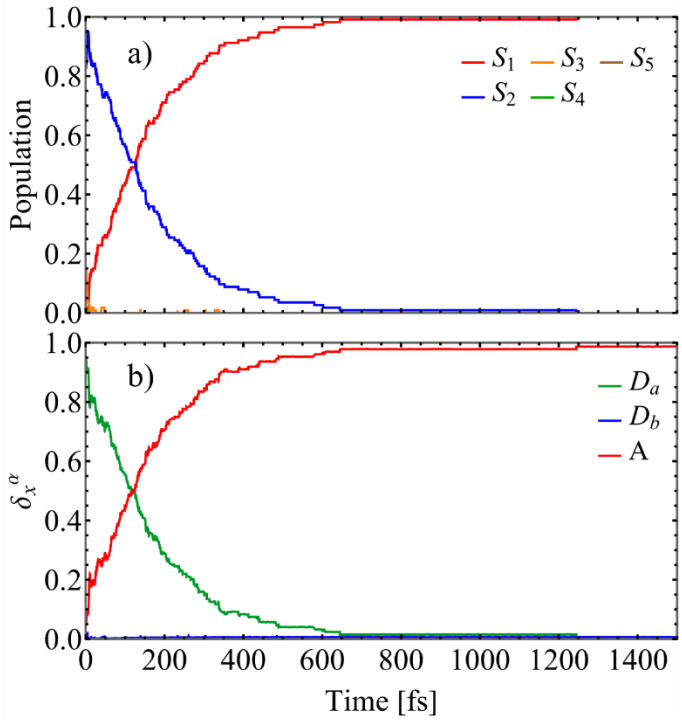

Figure S4. Analysis of trajectories following the direct $D_a \rightarrow$ A energy transfer pathway (a) Evolution of average populations of electronic states calculated from the fraction of trajectories in a particular state at a given time after the initial laser excitation evaluated for trajectories following the direct $D_a \rightarrow$ A energy transfer pathway. (b) Evolution of the average fraction of the transition density $\delta_X^\alpha(t)$ on the donors ($D_{a/b}$) with the highest/lowest initial value of $\delta_X^\alpha(0)$, respectively, and the acceptor (A).

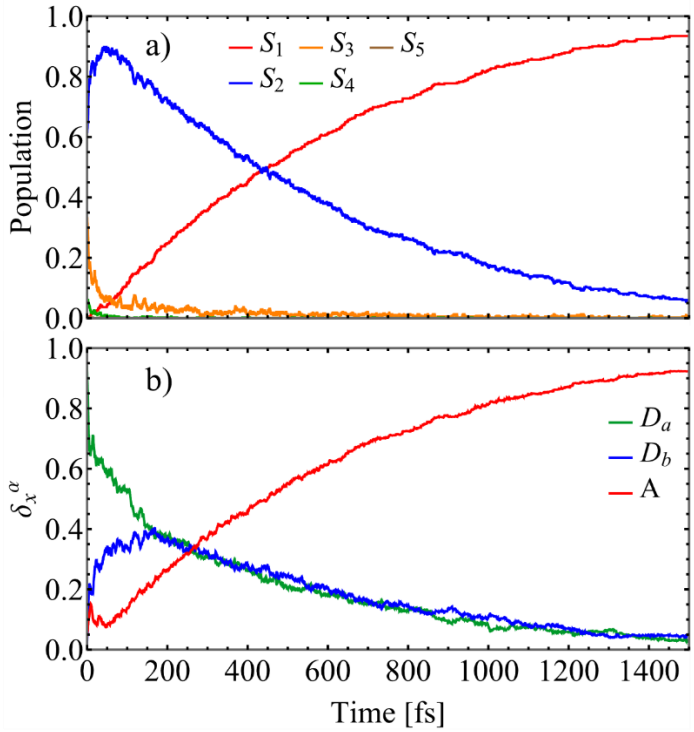

Figure S5. Analysis of trajectories following the indirect $D_a \rightarrow D_b \rightarrow A$ energy transfer pathway (a) Evolution of average populations of electronic states calculated from the fraction of trajectories in a particular state at a given time after the initial laser excitation evaluated for trajectories following the indirect $D_a \rightarrow D_b \rightarrow A$ energy transfer pathway. (b) Evolution of the average fraction of the transition density $\delta_X^\alpha(t)$ on the donors ($D_{a/b}$) with the highest/lowest initial value of $\delta_X^\alpha(0)$, respectively, and the acceptor (A).

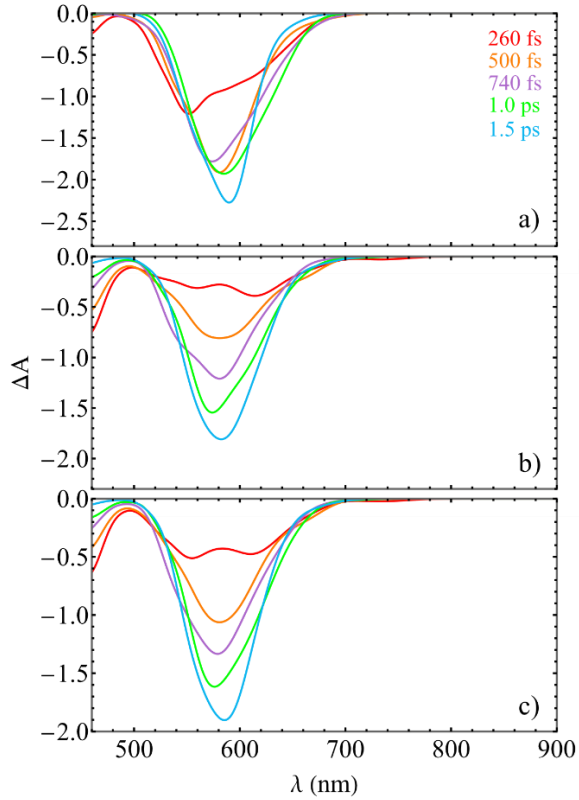

Figure S6. The SE contribution to the TA-PP signal $\overline{S_{int,\mathrm{M}}}(t, E_{pr})$ at different times. The data is averaged over trajectories corresponding to (a) the direct $D_a \rightarrow A$ energy transfer pathway, (b) the indirect $D_a \rightarrow D_b \rightarrow A$ energy transfer pathway, and (c) the overall set of trajectories.

Transition density flux analysis.

The transition density flux method enables monitoring of the different pathways of energy redistribution between chromophore units following the initial photoexcitation. Briefly, at each time interval Δt during the nonadiabatic simulations, the effective change in the transition density localized on unit X ($\delta_X^{\alpha}(t)$), denoted as $\Delta\delta_X(t)$ (with the superscript indicating the active state α omitted for clarity), is tracked using the flow matrix F(t). This matrix has zero-valued diagonal elements, while the off-diagonal elements $\mathrm{f_{XY}}(t)$ represent the amount of $\delta_X(t)$ transferred between units X and Y.

Chromophore units are classified as donors (D) when $\Delta\delta_X < 0$ and as acceptors (A) if $\Delta\delta_X > 0$. By applying the minimum flow criterion—which assumes that $\Delta\delta_X$ represents the minimal amount of effective transfer—we consider only the net transition density flows from donors to acceptors. The total transition density exchanged among units during the time interval Δt is given by:

$$\Delta\delta_{total}(\mathrm{t}) = \sum_{X\in D}\left|\Delta\delta_X(\mathrm{t})\right| = \sum_{Y\in A}\Delta\delta_Y(\mathrm{t}) \qquad \text{(S1)}$$

The flow elements $\mathrm{f_{XY}}(t)$ are antisymmetric, and thus calculated as:

$$\mathrm{f_{XY}}(t) = -\mathrm{f_{YX}}(t)$$

$$= \begin{cases} \dfrac{|\Delta\delta_X(t)|\Delta\delta_Y(t)}{\Delta\delta_{\mathrm{total}}(\mathrm{t})} & \mathrm{X} \in \mathrm{D}, \mathrm{Y} \in \mathrm{A} \\ 0 & \mathrm{X}, \mathrm{Y} \in \mathrm{D} \text{ or } \mathrm{X}, \mathrm{Y} \in \mathrm{A} \end{cases} \qquad \text{(S2)}$$

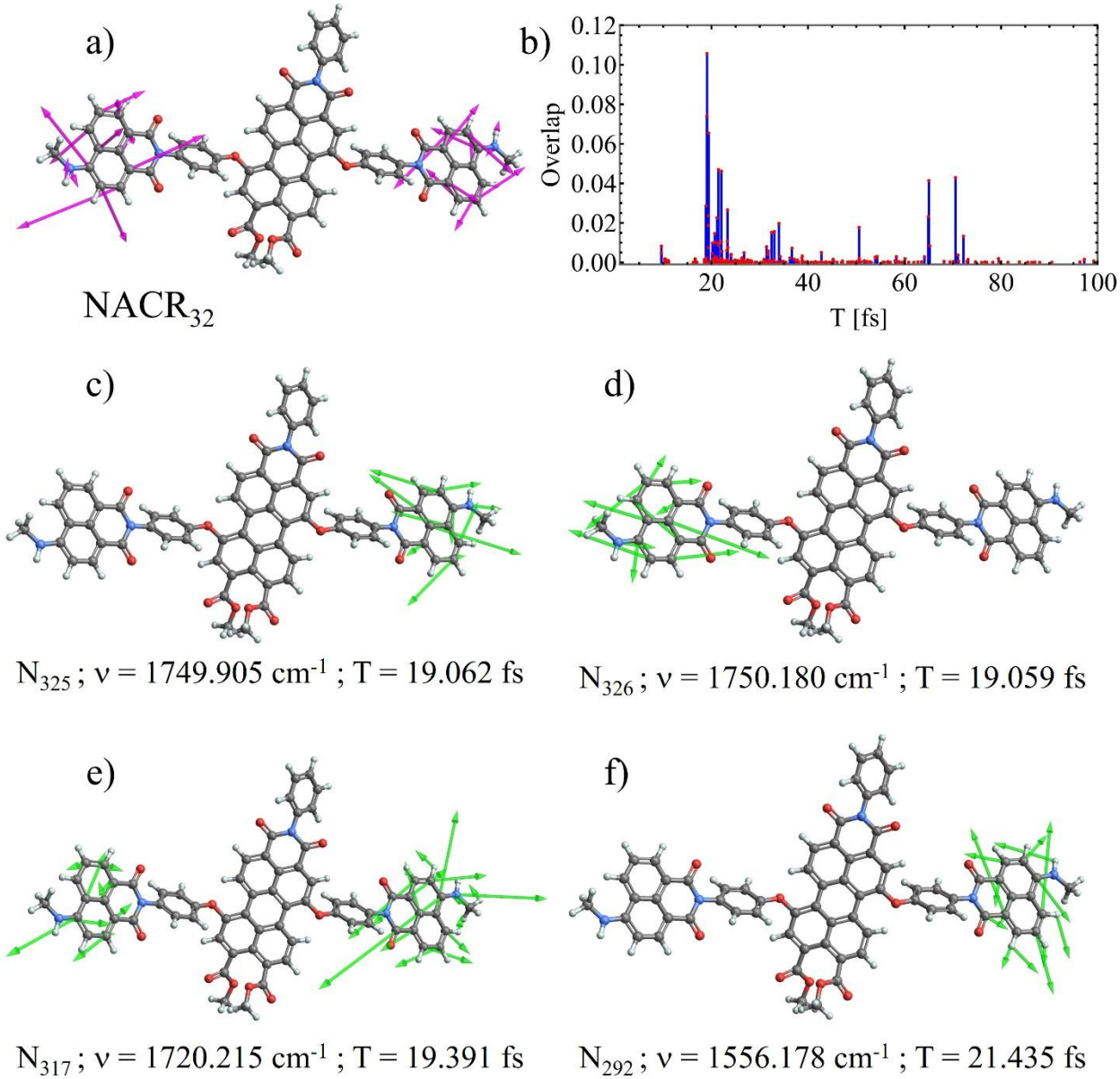

Figure S7. (a) Nonadiabatic coupling vector ($NACR_{32}$) associated to $S_3 \rightarrow S_2$ energy transfer: (b) overlaps of The projection of $NACR_{32}$ with the D2A2 normal modes: (c-f) Normal modes with the highest overlaps.

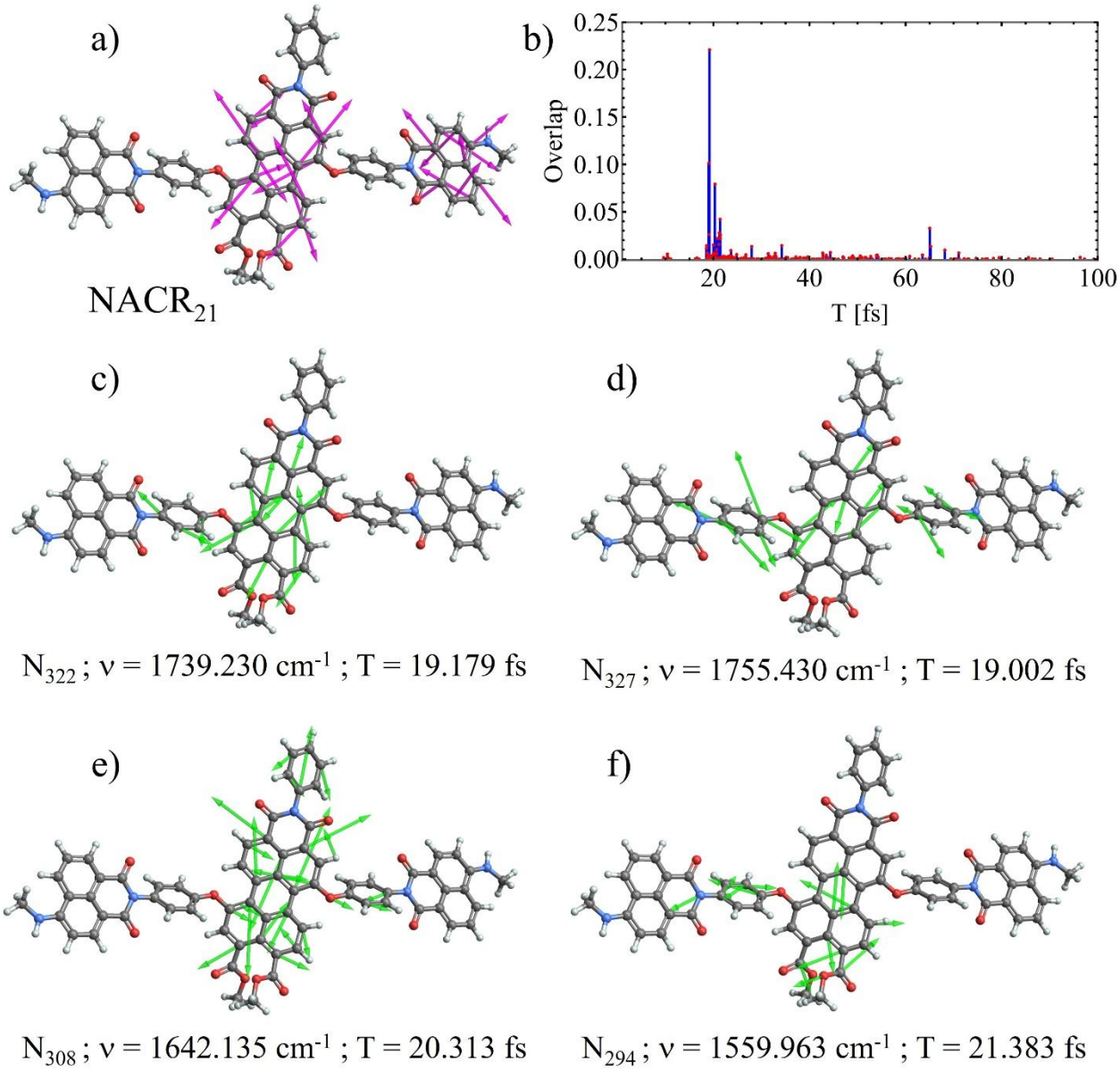

Figure S8. (a) Nonadiabatic coupling vector ($NACR_{21}$) associated to $S_2 \rightarrow S_1$ energy transfer: (b) overlaps of The projection of $NACR_{21}$ with the D2A2 normal modes: (c) Normal modes with the highest overlaps.